Conf-940552--43

UCRL-JC-117939
PREPRINT

A Numerical Study of Ultra-short-pulse Reflectometry

B.I. Cohen, B.B. Afeyan, A.E. Chou, and N.C. Luhmann, Jr.

This paper was prepared for submittal to the
Proceedings to the Tenth Topical Conference
on High Temperature Plasma Diagnostics
Rochester, NY
May 8-12, 1994

May 1994

Lawrence Livermore National Laboratory

DISCLAIMER

A Numerical Study of Ultra-short-pulse Reflectometry

B. I. Cohen,[1] B. B. Afeyan,[1] A. E. Chou,[2,3] and N. C. Luhmann, Jr.[3]

[1]Lawrence Livermore National Laboratory, University of California,
Livermore, California 94550
[2]Department of Electrical Engineering, University of California at Los Angeles
Los Angeles, California 90024
[3]Department of Applied Science, University of California at Davis
Livermore, California 94550

Abstract

Ultra-short-pulse reflectometry is studied by means of the numerical integration of a one-dimensional full-wave equation for ordinary modes propagating in a plasma. The numerical calculations illustrate the potential of using the reflection of ultra-short-pulse microwaves as an effective probe of the density profile even in the presence of significant density fluctuations. The difference in time delays of differing frequency components of the microwaves can be used to deduce the density profile. The modification of the reflected pulses in the presence of density fluctuations is examined and can be understood based on considerations of Bragg resonance. A simple and effective profile-reconstruction algorithm using the zero-crossings of the reflected pulse and subsequent Abel inversion is demonstrated. The robustness of the profile reconstruction algorithm in the presence of a sufficiently small amplitude density perturbation is assessed.

I. INTRODUCTION

Reflectometry has become a commonly used diagnostic for probing density profiles and fluctuations in laboratory plasmas. The primary reflectometry techniques have involved FM radar systems consisting of either a broadband swept-frequency source or a set of discrete narrowband frequency sources with matching multi-band detection systems.[1-3] This paper is motivated by the recent innovation of using moderate pulse ($\tau_p \approx 200$ ps) or ultra-short-pulse ($\tau_p \approx 1\text{-}3$ ps) microwave sources for advanced reflectometry applications.[4-8] It is hoped that pulsed techniques might be found useful in probing density profiles where swept-frequency sources with much longer sweep times have had difficulties.[9,10] Ultra-short-pulse reflectometry offers the advantages that a single short pulse replaces multiple microwave sources at discrete frequencies or a swept-frequency source, and many pulses can be launched and detected over a time interval that is short compared to the typical time scales on which the plasma density and other profiles of interest evolve.

In ultra-short-pulse reflectometry, a very short pulse of microwaves is propagated into a spatially nonuniform plasma. The pulse has a frequency content governed by the shape and duration of the pulse. Because the reflection of an ordinary mode of a given frequency occurs where the local plasma frequency (which depends on the square-root of the electron density) equals the mode frequency, the various frequency components comprising a short pulse will be reflected by plasma layers of differing density and will experience differing time delays in returning back to a detector located in or near the microwave launching structure. From the observed relation between the frequency components and the corresponding time or phase delays, the plasma density profile can be inferred using asymptotic methods, such as Wentzel-Kramers-Brillouin-Jeffreys (WKBJ) theory and an Abel inversion as in conventional swept-frequency reflectometry.[11,12] The validity of such a procedure can be checked by comparison with a direct numerical integration of the wave equation, and the experimental results can be checked by comparison with alternative diagnostic measurements of the density profile. However, the conventional phase integral and WKBJ techniques are unable to address the scattering of the electromagnetic waves in the presence of fluctuations localized near the reflection layer of the electromagnetic waves. In this case, the Born approximation may be used to model reflectometry for small amplitude fluctuations;[11] and direct numerical solutions of a full-wave equation also have been undertaken.[12,13,14] The work in Ref. 14 provides a comprehensive study of a direct numerical solution of a one-dimensional wave equation, while Ref. 15 presents a complete analytical treatment based on the Born approximation of wave scattering by fluctuations. The validity limits of the analysis in Ref. 15 are delineated in Ref. 14, and extensions beyond the Born approximation are obtained.

Research on short-pulse and ultra-short-pulse reflectometry has focused on the challenging technology aspects, the design and operation of the systems, and proof-of-principle experiments. There has been little or no analysis and modeling specific to short-pulse reflectometry. Here we present the results of one-dimensional numerical solutions of a full-wave equation describing the propagation and reflection of a short pulse of ordinary modes in a spatially nonuniform plasma. Our numerical studies address the influence of density fluctuations on the reflected pulse. The reflected pulse is spatially broadened by the spatially nonuniform density profile. The phase of a frequency component within the pulse is linearly perturbed by a small-amplitude fluctuation of a given wavelength if the Bragg resonance condition is satisfied (if the wavenumber of the density fluctuation is twice the local wavenumber of a frequency component of the probing microwaves at a particular density in the plasma). When the density fluctuation amplitude becomes large, the scattering of the microwaves by the density fluctuation is more pronounced; and distortion of the reflected pulse occurs. The numerical solution of the full-wave equation can treat this when the Born approximations would have failed. Although the reflected pulse can be significantly distorted by scattering from density fluctuations, our results indicate that the spreading of the pulse may still provide a useful measure of the background density gradient and that accurate profile reconstruction is possible for weak enough fluctuations.

We present several numerical examples illustrating pulsed reflectometry and the effects of density fluctuations in Sec. II. Conclusions and questions for future research are offered in Sec. III.

II. NUMERICAL MODELING OF ULTRA-SHORT-PULSE REFLECTOMETRY

The one-dimensional numerical calculations presented here illustrate fundamental aspects of ultra-short-pulse reflectometry. We have numerically integrated the one-dimensional wave equation for an ordinary mode in a plasma with an adjacent vacuum:

$$\left[\frac{\partial^2}{\partial t^2} - c^2\frac{\partial^2}{\partial x^2} + \omega_{pe}{}^2(x)\right]E(x,t)=0 \qquad (1)$$

with specified initial conditions $E(x,t=0)$ and $(\partial/\partial t)E(x,t=0)=-c(\partial/\partial x)E(x,t=0)$ for a right-going pulse launched in vacuum and outgoing-wave boundary conditions. We have adopted a second-order-accurate, central differencing scheme to solve Eq.(1). In vacuum, the algorithm has dispersion given by $\omega=\pm kc$; and electromagnetic pulses propagate without numerical dispersion, dissipation, or artificial reflection by the grid. In the plasma there are discretization corrections to the wave dispersion that scale as $\omega_{pe}^2\Delta t^2$ and $k^2\Delta x^2$. A more detailed elaboration of the numerical method used here and additional numerical examples are presented in Ref. 16.

In all of the examples, a highly localized pulse, $E(x,t=0) = \exp[-(x-x_p)^2/\tau_p^2]$, is initialized in the vacuum region (see Fig. 1) and propagated into a monotonically increasing electron density profile. The density profile chosen is $n_e(x) = n_o \exp[(x-x_o)/L_s]$ for $x<x_o$ and $n_e(x) = n_o [1+(x-x_o)/L_s]$ for $x\geq x_o$, where x_o is a reference point to the right of x_p, n_o is a reference electron density, and L_s is a scale length. With this choice, the density profile is smooth and is linear over most of a domain within which we can locate density fluctuations at different positions. The parameters of physical interest are the ratios L_s/τ_p and n_o/n_c, where n_c is the density where the local plasma frequency $\omega_{pe}=(4\pi n_c e^2/m_e)^{1/2}$ equals a characteristic frequency of the pulse, e.g., $\omega_o=\pi/2\tau_p$. The shortest length scale in the computation is τ_p, which is set equal to 20 Δx ($\Delta x=\Delta t=c=1$ in our units) to ensure adequate resolution in all of the cases reported.

In Fig. 1 we present the results of a numerical calculation of the reflection of an ultra-short pulse by a monotonically increasing plasma density profile. The density scale length $L_s=120$, and $n_o=n_c$. The initial pulse and the electron density profile are shown in Fig. 1(a), and the reflected pulse is shown in Fig. 1(b) along with the Fourier spectrum computed from E(x,t). The frequency half-width at half-maximum of the initial pulse is $\omega_{1/2}\approx 0.1\approx 2\pi/3\tau_p$, and the Fourier amplitudes of the pulse are <1% of the maximum at $\omega=0$ for $\omega>2\pi/\tau_p$. We note that the pulse is significantly dispersed by the reflection process. The lowest-frequency components return first, because they are reflected first from the lowest densities; and the higher-frequency components experience increasingly longer delays. If we take as an effective maximum frequency component of the pulse $\omega_{max}=2\pi/\tau_p$, this highest-frequency component of the pulse will travel a distance approximately equal to $(\omega_{max}/\omega_o)^2 L_s$ farther into a linear plasma profile than will the lowest frequency component. Thus, the reflected pulse will be broadened to a full width given approximately by $\tau_r \sim 2(\omega_{max}/\omega_o)^2 L_s$, which is ~3800 in this case and is in fair agreement with the numerical calculation. With a more detailed analysis of the time delays of the frequency components of the pulse presented later in the paper, we are able to make additional inferences regarding monotonic plasma density profiles.

An electromagnetic wave can be scattered by a density fluctuation under certain circumstances. Linear perturbation theory, in particular, the Born approximation (see Ref. 15, and references therein), can be used to solve Eq.(1) perturbatively to deduce the effect of a small-amplitude density fluctuation. The lowest-order solution ignores the density fluctuation in Eq.(1) to obtain $E^{(0)}$. In first Born approximation, the perturbation $E^{(1)}$ satisfies an equation like Eq.(1) with just the unperturbed plasma density on the left side in the term $\omega_{p0}^2 E^{(1)}$ and a source term on the right side containing the beat of the perturbed density due to the fluctuation with the lowest order electromagnetic field, $-\delta\omega_p^2 E^{(0)}$,

$$\left[\frac{\partial^2}{\partial t^2} - c^2 \frac{\partial^2}{\partial x^2} + \omega_{p0}^2\right] E^{(1)} = -\delta\omega_p^2 E^{(0)} \qquad (2)$$

Consideration of this inhomogeneous wave equation for $E^{(1)}$ leads to the following observations. A finite-wavelength fluctuation can beat resonantly with $E^{(0)}$ to produce a scattered wave $E^{(1)}$ that satisfies the local dispersion relation if a resonance condition is satisfied. From an asymptotic point of view, the one-dimensional resonance condition is

$$\pm k(x) \pm k_f = -k(x), \qquad (3)$$

so that a scattered wave with wavenumber $-k(x)$ will propagate back to a detector placed at the source. Here, k_f is the fluctuation wavenumber, and $k(x)$ is the wavenumber of the electromagnetic wave satisfying the local dispersion relation $\omega^2 = k(x)^2 c^2 + \omega_{pe}^2(x)$. Thus, a photon propagating up the gradient can be backscattered by a fluctuation into a photon propagating down the gradient when the Bragg resonance condition (see Ref. 15 and references therein) is satsified:

$$k_f = 2k(x) = 2[\omega^2 - \omega_{pe}^2(x)]^{1/2}/c \qquad (4)$$

For an ultra-short pulse, there is a range of frequency components (effectively up to $\omega_{max} = 2\pi/\tau_p$). We deduce from Eq.(4) that Bragg resonance is possible somewhere in the plasma for some frequency component of the ultra-short pulse when $k_f \leq 2\omega_{max}/c$.

To examine the effects of the scattering by density fluctuations on reflectometry, we superposed on the plasma density profile a coherent localized density perturbation modeled by $\delta n(x) = \delta n_o \exp[-(x-x_c)^2/x_w^2] \cos[k_f(x-x_c)]$. We have undertaken integrations of Eq.(1) for various $\delta n_o/n_o$. With $k_f > 2\omega_{max}/c$ chosen to preclude Bragg resonance, and for small $\delta n_o/n_o$, there was no discernible scattering; and the reflected pulse was unperturbed. For $k_f < 2\omega_{max}/c$ and x_c located within the plasma at a density corresponding to $\omega_{pe}(x_c) \leq \omega_{max}$, the Bragg resonance condition can be satisfied; and for $\delta n_o/n_o \ll 1$, we observed small perturbations in the reflected pulse in consequence of the scattering (Fig. 2). In other examples, we changed the value of x_c, the location of the center of the density perturbation. For a fixed value of k_f, localizing the fluctuation to larger values of x_c, which corresponded to higher plasma densities, forced the resonant frequency components of the pulse to higher values of ω to satisfy Eq.(4).[16] We also studied the effect of changing the fluctuation wavenumber. The theory presented in Ref. 15 gives an expression for the scattering phase shift and shows that it is modulated as a function of the position of the center of the density perturbation x_c with a wavenumber k_f for $k_f x_w >> 1$. This spatial modulation maps into the frequency modulation observed in the plot of the tangent of the scattering phase shift vs. frequency because of the Bragg resonance condition, Eq.(4), for fixed k_f.[16] Reference 15 also concludes that the amplitude of the phase shift depends on $k_f^{-1/2}$ and that the overall width in space (or frequency in Fig. 2) is determined mainly by x_w. These parametric dependences are confirmed in the numerical examples of ultra-short pulse reflectometry reported by us in Ref. 16.

For small-amplitude fluctuations, the perturbations in the reflected electric field due to the scattered wave $E^{(1)}$ can be iterated to higher order to obtain additional corrections within the Born approximation. This yields a power series in the appropriately scaled amplitude of the density perturbation,[15] the first term of which corresponds to the first Born approximation, Eq.(2). The higher-order terms satisfy their own resonance conditions. Thus, the scattering and pulse distortion increase in both magnitude and complexity as the amplitude of the density perturbation increases. For sufficiently large amplitudes, the Born approximation fails;[14] and the pulse propagation and reflection become quite complex. For example, tunneling and multiple reflection can occur.

Figures 2 and 3 display results for $k_f = 0.25\omega_{max}/c$, $x_w=L_s$, $x_c=x_o+L_s$, and $\delta n_o/n_o=0.2$ and 0.4, respectively. The distortion of the reflected pulses and the scattering phase shifts increase with the amplitude $\delta n_o/n_o$, and the dependence of the phase shift on frequency deviates significantly from a sinusoid with a Gaussian envelope for $\delta n_o/n_o=0.4$. However, the overall length of the reflected pulses, from which the slope of the unperturbed plasma profile can be inferred, does not appear to be very much altered from the case with no fluctuations in Fig. 1. The density perturbation $\delta n_o/n_o=0.2$ corresponds to a normalized amplitude $(\delta n_o/n_o)(k_o L_s)^{2/3}=0.9$ where $k_o=\omega_{max}/4$. The results of Ref. 14 indicate that when the normalized density perturbation approaches a value of unity, the first Born approximation begins to fail significantly.

A monotonically increasing plasma density profile can be reconstructed from a reflected pulse using the following prescription. If the density scale length of the plasma is much longer than the typical vacuum wavelength of the microwaves in the pulse, the geometric optics approximation may be applied to the calculation of the time delays of the various frequency components.[1] The time delay for a wave with a frequency ω to propagate from a position x=0 to its reflection point at $x=x_r$, where $\omega=\omega_{pe}$, is given approximately by

$$\tau(\omega) = \int_0^{x_r} dx \frac{2}{v_g} = \int_0^{x_r} dx \frac{2\omega}{k(x)c^2} = \int_0^{x_r} dx \frac{2}{c}\left[1 - \frac{\omega_{pe}^2(x)}{\omega^2}\right]^{-1/2} \qquad (5)$$

For a monotonic density profile, Eq.(6) can be Abel inverted to obtain[1]

$$x(\omega_{pe}) = \int_0^{\omega_{pe}} d\omega \, \frac{c\tau(\omega)}{\pi(\omega_{pe}{}^2-\omega^2)^{1/2}} = \int_0^{\pi/2} d\theta \, \frac{c\tau(\omega=\omega_{pe}\sin\theta)}{\pi} \qquad (6)$$

Equation (6) can be used to map ω_{pe} as a function of x given a knowledge of the time delays as a function of frequency. It is important to note that Eq.(6) only determines the location x corresponding to ω_{pe} relative to the edge of the plasma. Additional knowledge of the plasma density at a single point serves as a boundary condition that fixes the location of the entire profile.

To use Eq.(6) to reconstruct the density profile, we have determined $\tau(\omega)$ from the zero crossings of E(x,t) in vacuum after the reflection of the pulse. In our integrations, we tabulate the times t_j for which E(x,t) changes sign for a prescribed x (or at fixed time, tabulate the positions of the zero crossings). Because the values of E(x,t) are determined only at discrete values of x and t, the zero crossings are computed by linear interpolation using successive values of E(x,t) that have changed sign. From the separation of successive zeros in time, $\Delta t=t_{j+1}-t_j$, we take as an *ansatz* that $\omega_j=\pi/\Delta t$ is the characteristic frequency associated with the time delay $\tau_j=(t_{j+1}+t_j)/2$. In order to ensure monotonicity, we sweep through the tabulated values of $\{\omega_j\}$ and reorder the data so that the $\{\omega_j\}$ are monotonically increasing before performing the integration in Eq.(6). This is equivalent to a smoothing of the data. We note that the density profile can be mapped over a density range, i.e., a range of plasma frequencies, corresponding to the range of frequencies in the pulse.

Figure 4 presents results for the application of Eqs.(5) and (6) to the integrations of the wave equation for two different values of $\delta n_o/n_o$ for a coherent density perturbation. The density profile obtained from Eq.(6) for the case of no fluctuation shown in Fig. 1 agrees quite well with the actual density, Fig. 4. The resolution of the density profile reconstruction is constrained by the limited number of zero crossings (~50) on which the integration in Eq.(7) is based. With a 10-20% density perturbation present, the unsmoothed time delays vs. frequency relations exhibit significant deviations from the case with no density perturbation. Nevertheless, the smoothed data lead to a density profile reconstruction that agrees quite well with the true unperturbed profile. For relative density perturbations equal to or greater than 40% that satisfy Bragg resonance with the pulse, the distortions to the reflected pulse are profound and the density-profile reconstruction fails badly except at low densities where there is no Bragg scattering for these cases. The density-profile reconstruction agrees with the unperturbed density profile with acceptable accuracy (error <10%) for density perturbations up to 20% relative magnitude. This density perturbation corresponds to a normalized amplitude $(\delta n_o/n_o)(k_oL_s)^{2/3}$=0.9 where $k_o=\omega_{max}/4$. Reference 15 first identified this parameter to be the dominant one in controlling the applicability of the Born approximation. The numerical calculations of Ref. 14 corroborate this and show that the Born approximation fails only after this normalized density variable becomes of O(1).

An additional series of computations was performed with superposed density perturbations of the form $\delta n(x) = \delta n_o \exp[-(x-x_c)^2/x_w^2]\ \Sigma_i a_i \cos[k_i(x-x_c)]$, where there were four terms in the sum, a_i=0.25, $\{k_i/k_f\}$={0.17, 0.37, 0.63, 0.88}, and k_f = $0.25\omega_{max}/c$. Figure 5 displays the results of a computation with $\delta n_o/n_o$=0.25. There is significant evidence of Bragg resonance and relatively strong scattering. However, the reconstruction of the density profile is quite good over the range of plasma densities accessible to the pulse subject to the monotonicity constraint.

III. CONCLUSIONS

In this paper we have studied the propagation and reflection of an ultra-short pulse of ordinary modes and their scattering by density fluctuations in a nonuniform plasma. We have demonstrated how the plasma density profile can be reconstructed from information contained in the reflected pulse using a simple algorithm. The numerical examples presented illustrate the basic principle of ultra-short-pulse reflectometry in the absence of significant density fluctuations and how density fluctuations modify the reflected pulse within the restrictions of a one-dimensional model.

Our calculations demonstrate that an analysis of the Fourier spectrum taking into account Bragg resonance leads to an understanding of the effects of scattering by density fluctuations on the reflected pulses. For small-amplitude density fluctuations, it appears possible to reconstruct the average density profile from the information contained in the reflected pulse and to infer some of the characteristics of the superposed density fluctuations as well. For large-amplitude fluctuations that are Bragg resonant with the pulse, there is significant distortion of the reflected pulse; and the propagation and reflection process is much more complex. We speculate that by making multiple short-pulse reflectometry measurements, one may be able to average away some of the effects of scattering by density fluctuations. Alternatively, a smoothing of the time delay vs. frequency data based on a correlation analysis of the various components of the reflected pulse, in which the large, uncorrelated distortions of the reflected pulse due to large-amplitude fluctuations could be systematically removed, might salvage the profile-reconstruction algorithm.

The calculations presented here have been strictly one-dimensional. Elsewhere we have studied in detail the influence of multi-dimensional scattering and interference effects on reflectometry, and have addressed the important issue of apparent localization in using reflectometry to measure density fluctuations.[17] Both multi-dimensional effects and the use of extraordinary-mode short pulses are important for laboratory applications and will be addressed in future calculations.

We are grateful to Dr. E. A. Williams for his advice and encouragement, and to Dr. C. W. Domier for his technical input and interest in this research. This work was supported by the U.S. Department of Energy under Contract Nos. W-7405-ENG-48 and DE-FG03-86-ER53225 at the Lawrence Livermore National Laboratory and the Department of Applied Science, University of California at Davis.

References

[1]J.L. Doane, E. Mazzucato, and G.L. Schmidt, Rev. Sci. Instum. **52**, 12 (1981).

[2]F. Simonet, Rev. Sci. Instrum. **56**, 664 (1985).

[3]A.C.C. Sips and G.J. Kramer, Plasma Phys. Contr. Fusion **35**, Plasma Phys. Control Fusion **35**, 743 (1993).

[4]C.W. Domier, E. Chung, E.J. Doyle, H.-X.L. Liu, A. Lapidus, N.C. Luhmann, Jr., W.A. Peebles, X.-H. Qin, T.L. Rhodes, and L. Sjogren, Rev. Sci. Instum. **63**, 4666 (1992).

[5]V.F. Shevchenko, A.A. Petrov, and V.G. Petrov, International Jrnl of Infrared and Millimeter Waves **14**, 1755 (1993).

[6]N.C. Luhmann, Jr. et al., *Diagnostics for Contemporary Fusion Experiments* (Societa Italiana di Fisica, Varenna, Italy, 1991), pp. 135-178; B. Branas, T. Estrada, P. de la Luna, and A.P. Navarro, *Diagnostics for Contemporary Fusion Experiments* (Societa Italiana di Fisica, Varenna, Italy, 1991), pp. 739-746.

[7]V.A. Vershkov and V.A. Zhuravlev, Sov. Phys, Sov. Phys. Tech. Phys. **32**, 523 (1987).

[8]C.A.J. Hugenholtz and S. H. Heijnen, Rev. Sci. Instum. **62**, 1100 (1991).

[9]T. Lehecka, W.A. Peebles, N.C. Luhmann, Jr., S.R. Burns, E. Olson, and the DIII-D Group, Rev. Sci Instrum. **59**, 1620 (1988).

[10]E.J. Doyle T. Lehecka, N.C. Luhmann, Jr., W.A. Peebles, and the DIII-D Group, Rev. Sci. Instrum. **61**, 2896 (1990).

[11]I.H. Hutchinson, *Principles of Plasma Diagnostics* (Cambridge: Cambridge University

Press),1987; I.H. Hutchinson, Plasma Phys. Control. Fusion **34**, 1225 (1992); and references therein.

[12]N.Bretz, Phys. Fluids B **4**, 2414 (1992).

[13]J.H. Irby, S. Horne, I.H. Hutchinson and P.C. Stek, Plasma Phys. Control. Fusion **35**, 601 (1993).

[14]A.E. Chou, B.B. Afeyan, B.I. Cohen, and N.C. Luhmann, Jr., submitted to Rev. Sci. ..Instrum.; A.E. Chou, B.B. Afeyan, B.I. Cohen, and N.C. Luhmann, Jr., Plasma Phys. Control. Fusion.

[15]B.B. Afeyan, A.E. Chou, and B.I. Cohen, submitted to Plasma Phys. Control. Fusion.

[16]B.I. Cohen, B.B. Afeyan, A.E. Chou, and N.C. Luhmann, Jr., submitted to Plasma Phys. Control. Fusion.

[17]B.B. Afeyan, B.I. Cohen, and E.A. Williams, to be submitted to Plasma Phys. Control. Fusion.

Figure Captions

Figure 1. Pulse propagation and reflection with no density fluctuations present. (a) The initial configurations of the electromagnetic pulse and the plasma density (ω_{pe}^2 is plotted) as functions of position. (b) The reflected electromagnetic pulse vs. x at t=3000. (c) The moduli of the Fourier coefficients of the initial (1) and reflected (2) pulses as a function of frequency/wavenumber. (d) The tangent of the phase of the complex Fourier amplitudes of the reflected pulse as a function of frequency/wavenumber.

Figure 2. Pulse propagation and reflection with density fluctuations present: $\delta n_o/n_o=0.2$, $k_f = 0.5\pi/\tau_p$, $x_w=L_s$, and $x_c=x_o+L_s$. (a) The initial configurations of the electromagnetic pulse and plasma density as functions of position. (b) The reflected electromagnetic pulse vs. x at t=3000. (c) The moduli of the Fourier coefficients of the initial (1) and reflected (2) pulses as a function of frequency/wavenumber. (d) The tangent of the scattering phase shifts of the complex Fourier amplitudes of the reflected pulse as a function of frequency/wavenumber.

Figure 3. Pulse propagation and reflection with density fluctuations present: $\delta n_o/n_o=0.4$, $k_f = 0.5\pi/\tau_p$, $x_w=L_s$, and $x_c=x_o+L_s$. (a) The initial configurations of the electromagnetic pulse and plasma density as functions of position. (b) The reflected electromagnetic pulse vs. x at t=3000. (c) The moduli of the Fourier coefficients of the initial (1) and reflected (2) pulses as a function of frequency/wavenumber. (d) The tangent of the scattering phase

shifts of the complex Fourier amplitudes of the reflected pulse as a function of frequency/wavenumber.

Figure 4. Density-profile reconstructions. (a) Time delays τ vs. ω. (b) Reordered ("smoothed") time delays τ vs. ω. (c) True (1) and reconstructed (2) plasma densities ω_{pe}^2 vs. x. Data for $\delta n_o/n_o=0$ are shown above that for $\delta n_o/n_o=0.2$.

Figure 5. Pulse propagation and reflection with a multi-mode density fluctuation present: $\delta n_o/n_o=0.25$, $x_w=2L_s$, and $x_c=x_o+L_s$. (a) The reflected electromagnetic pulse vs. x at t=3000. (b) True (1) and reconstructed (2) plasma densities ω_{pe}^2 vs. x.

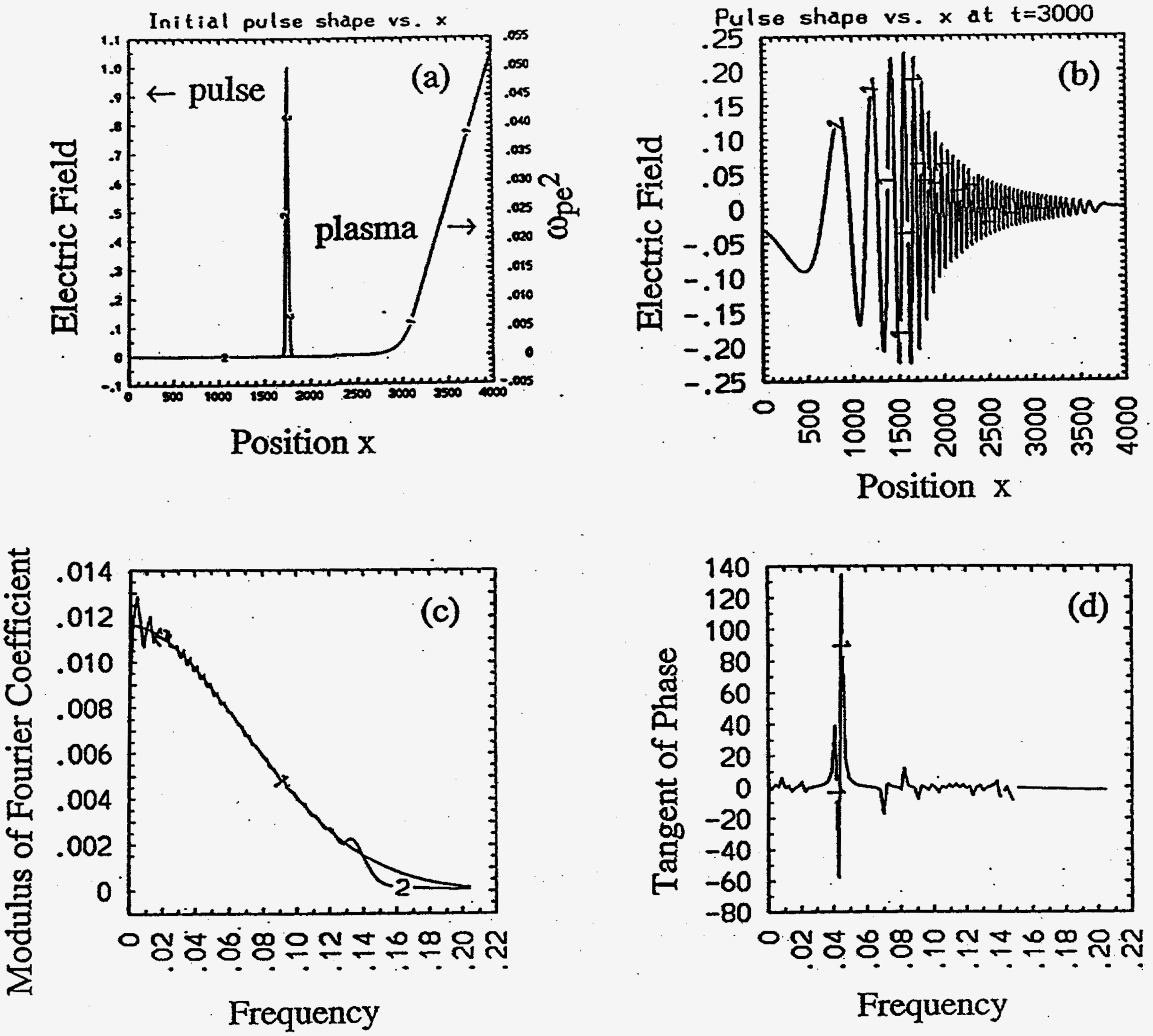

Initial pulse shape vs. x
(a)
← pulse
plasma →
Electric Field
ω_{pe}^2
Position x
Pulse shape vs. x at t=3000
(b)
Electric Field
Position x
(c)
Modulus of Fourier Coefficient
Frequency
(d)
Tangent of Phase
Frequency

Figure 1

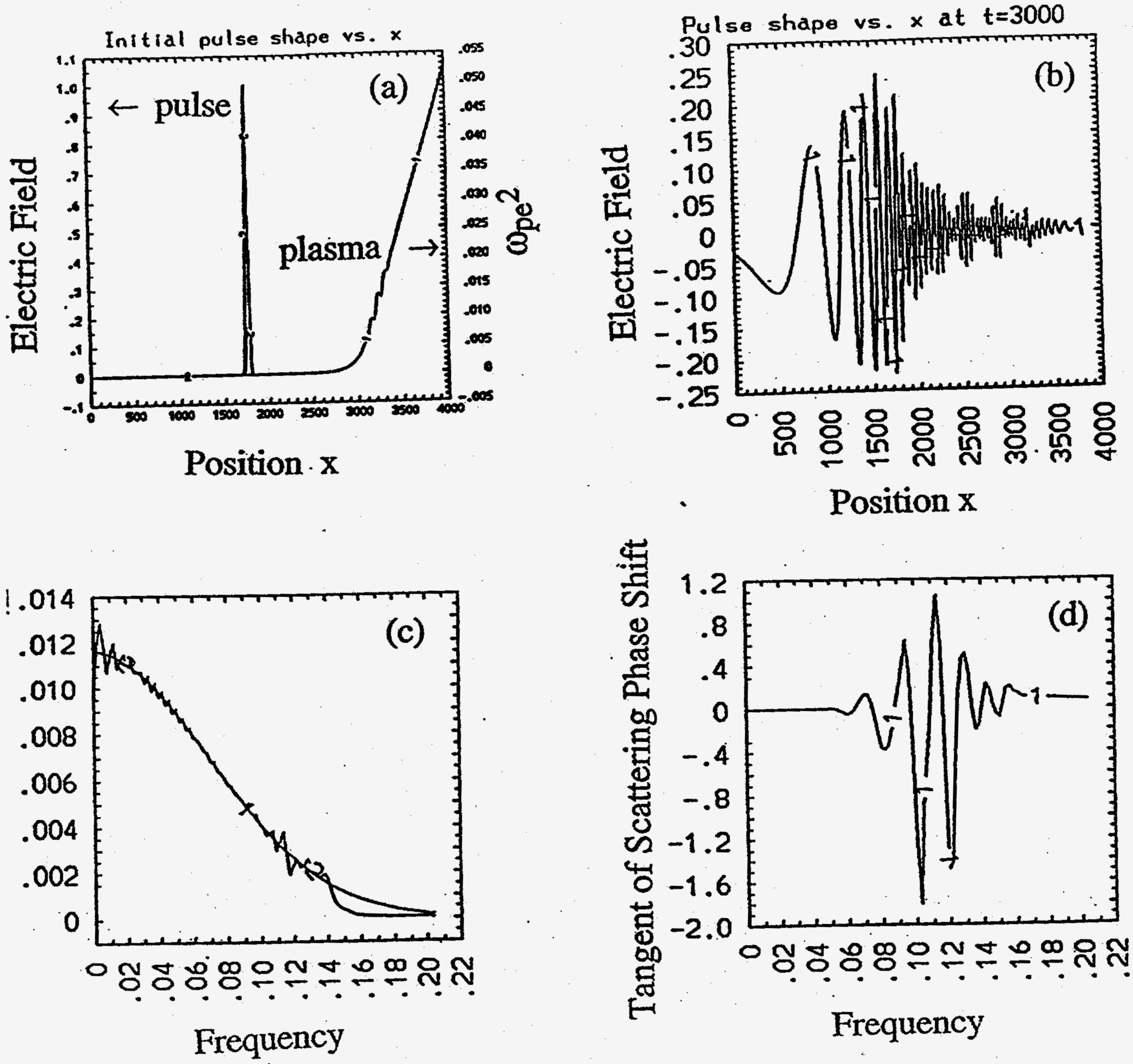
Initial pulse shape vs. x
(a)
← pulse
plasma →
Electric Field
ω_{pe}^2
Position x
Pulse shape vs. x at t=3000
(b)
Electric Field
Position x
(c)
Modulus of Fourier Coefficient
Frequency
(d)
Tangent of Scattering Phase Shift
Frequency

Figure 2

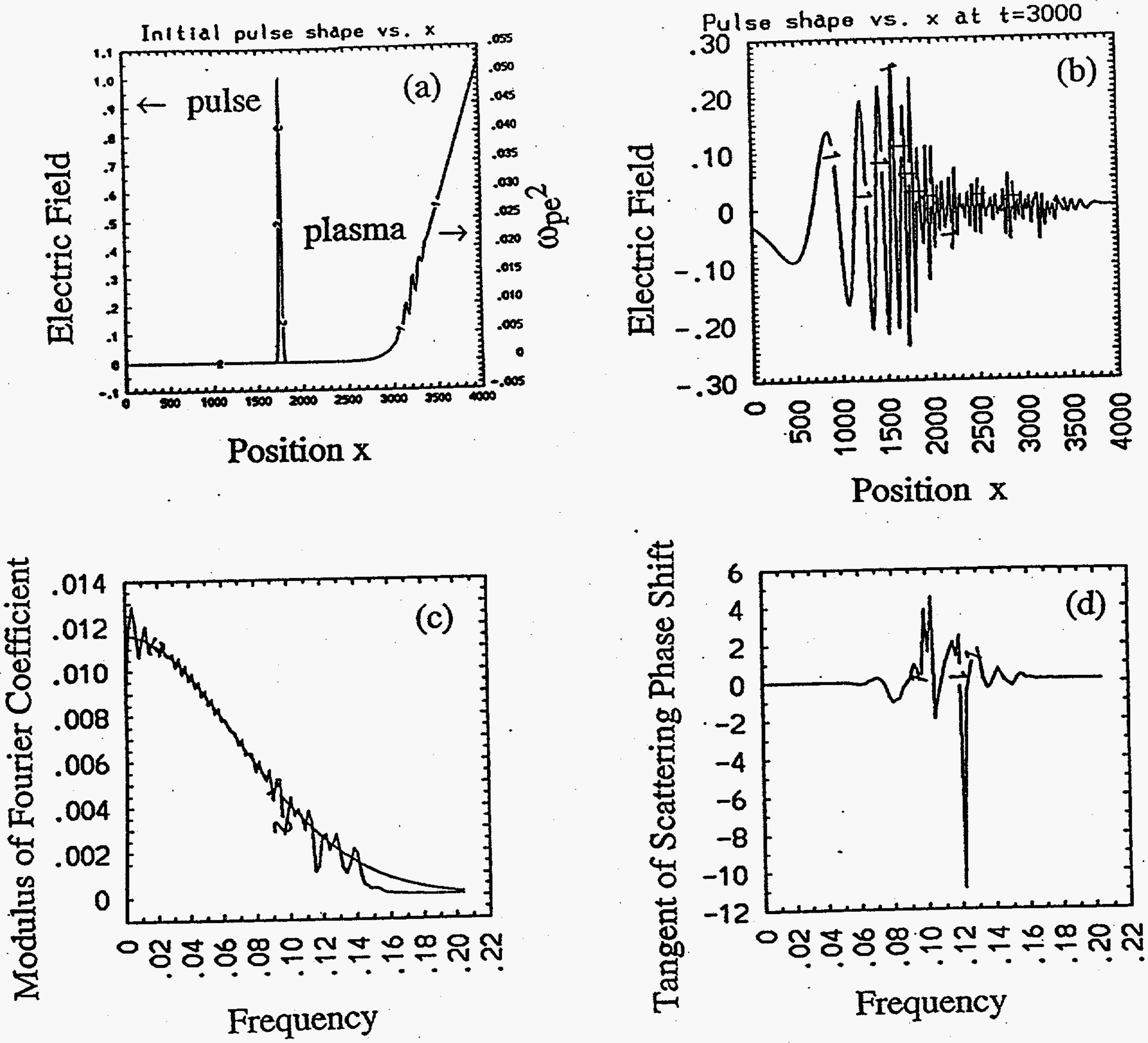

Initial pulse shape vs. x
← pulse
plasma →
(a)
Electric Field
ω_{pe}^2
Position x
Pulse shape vs. x at t=3000
(b)
Electric Field
Position x
(c)
Modulus of Fourier Coefficient
Frequency
(d)
Tangent of Scattering Phase Shift
Frequency

Figure 3

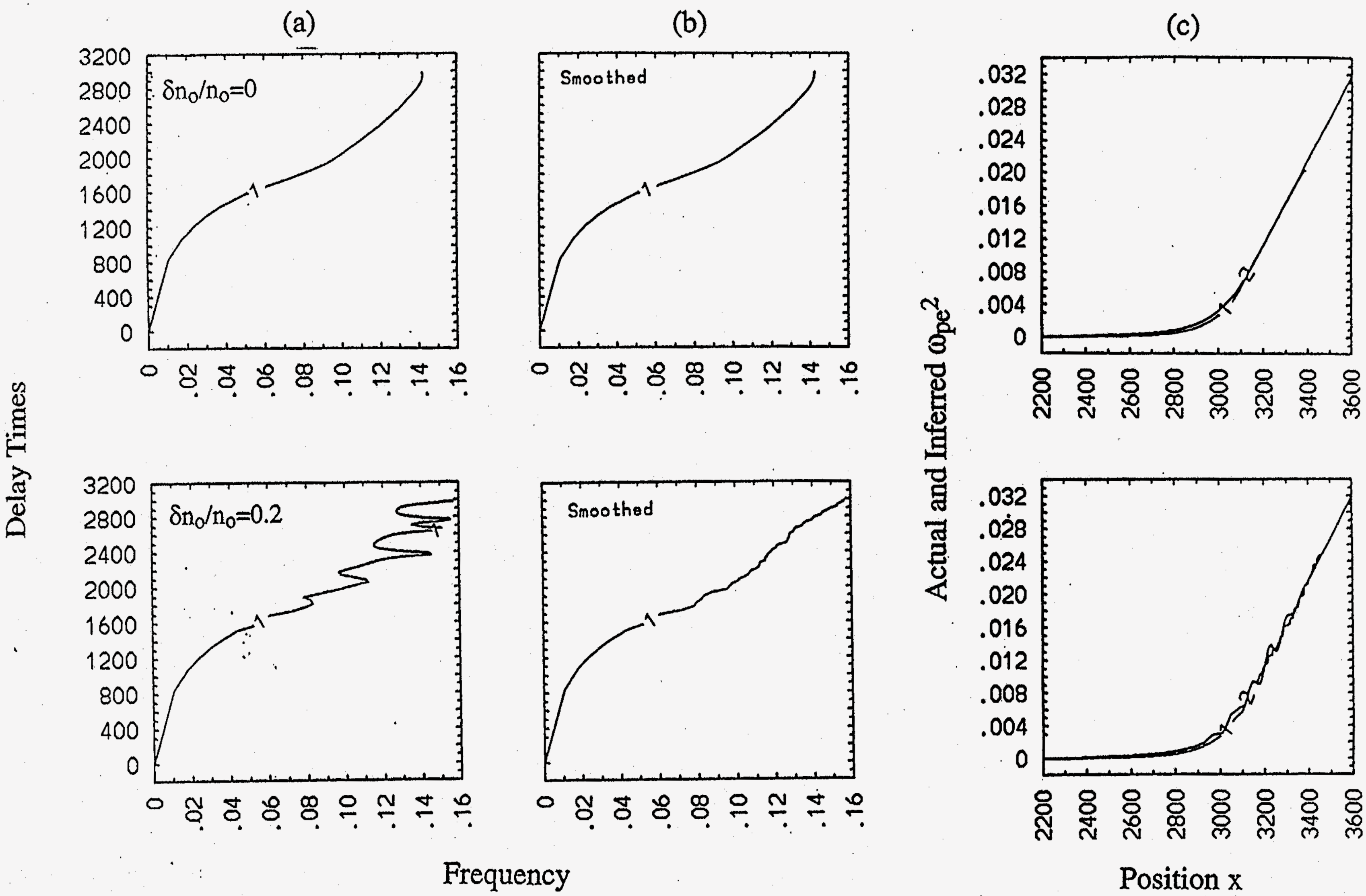

(a)
(b)
(c)
Delay Times
Frequency
Actual and Inferred ω_{pe}^2
Position x
$\delta n_o/n_o$=0
$\delta n_o/n_o$=0.2
Smoothed
Smoothed

Figure 4

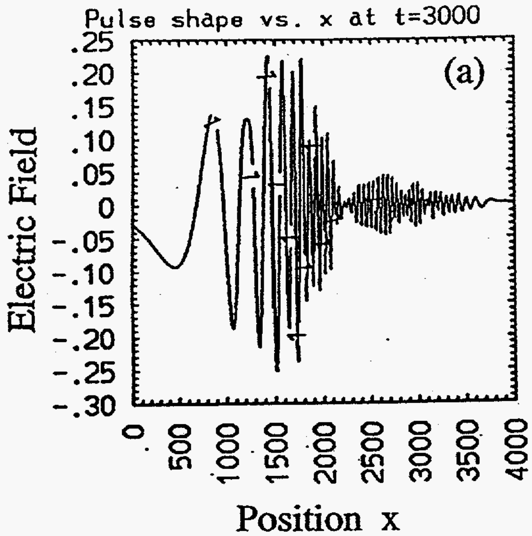

Pulse shape vs. x at t=3000
(a)
Electric Field
.25
.20
.15
.10
.05
0
-.05
-.10
-.15
-.20
-.25
-.30
0
500
1000
1500
2000
2500
3000
3500
4000
Position x

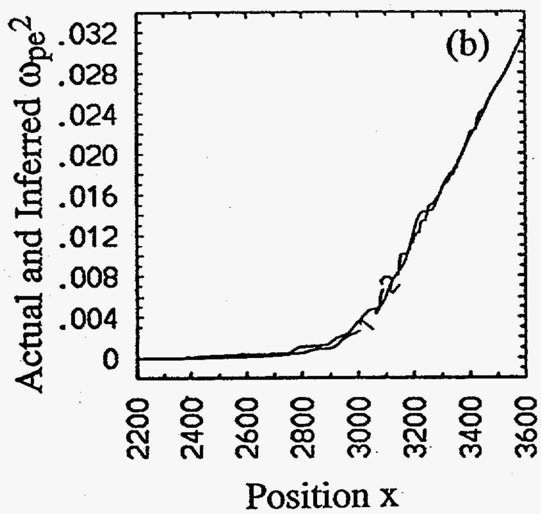

(b)
Actual and Inferred ω_{pe}^2
.032
.028
.024
.020
.016
.012
.008
.004
0
2200
2400
2600
2800
3000
3200
3400
3600
Position x

Figure 5